J. Biochem. 2012;151(5):533–540 doi:10.1093/jb/mvs025

JB THE JOURNAL OF BIOCHEMISTRY

Interaction of 8-anilinonaphthalene 1-sulphonate (ANS) and human matrix metalloproteinase 7 (MMP-7) as examined by MMP-7 activity and ANS fluorescence

Received December 19, 2011; accepted January 18, 2012; published online March 5, 2012

Vimbai Samukange, Kiyoshi Yasukawa and Kuniyo Inouye*

Division of Food Science and Biotechnology, Graduate School of Agriculture, Kyoto University, Sakyo-ku, Kyoto 606-8502, Japan

*Kuniyo Inouye, Division of Food Science and Biotechnology, Graduate School of Agriculture, Kyoto University, Sakyo-ku, Kyoto 606-8502, Japan. Tel: +81-75-753-6266, Fax: +81-75-753-6265, email: inouye@kais.kyoto-u.ac.jp

Human matrix metalloproteinase 7 (MMP-7) is the smallest matrix metalloproteinase. It plays important roles in tumour invasion and metastasis. 8-Anilinonaphthalene 1-sulphonate (ANS) is a fluorescent probe widely used for the analysis of proteins. It emits large fluorescence energy when its anilinonaphthalene group binds with hydrophobic regions of protein. In this study, we analysed the interaction of ANS and MMP-7. At pH 4.5–9.5, ANS inhibited MMP-7 activity in the hydrolysis of (7-methoxycoumarin-4-yl)acetyl–L-Pro–L-Leu–Gly–L-Leu-[N^3-(2,4-dinitrophenyl)-L-2,3-diaminopropionyl]–L-Ala–L-Arg–NH_2. The inhibition was a non-competitive manner and depended on the time for pre-incubation of ANS and MMP-7. At pH 4.5–9.5, the fluorescence of ANS was not changed by the addition of MMP-7. At pH 3.5, MMP-7 lacked activity, and the fluorescence of ANS was increased by the addition of MMP-7. These results suggest that at pH 4.5–9.5, the sulphonic group of ANS binds with MMP-7 through electrostatic interaction, whereas at pH 3.5, the anilinonaphthalene group of ANS binds with MMP-7 through hydrophobic interaction.

Keywords: ANS/fluorescence/inhibition/matrix metalloproteinase/MMP-7.

Abbreviations: AMPSO, 3-[(1,1-dimethyl-2-hydroxy-ethyl)amino]-2-hydroxypropane sulphonic acid; ANS, 8-anilinonaphthalene 1-sulphonate; *D*, dielectric constant; DMSO, dimethyl sulphoxide; HEPES, 2-[4-(2-hydroxyethyl)-1-piperazinyl] ethanesulphonic acid; MES, 2-(*N*-morpholino)ethanesulphonic acid; MMP, matrix metalloproteinase; MOCAc-PLG, (7-methoxycoumarin-4-yl) acetyl–L-Pro–L-Leu–Gly; MOCAc-PLGL(Dpa)AR, (7-methoxycoumarin-4-yl)acetyl–L-Pro–L-Leu–Gly–L-Leu- [N^3-(2,4-dinitrophenyl)-L-2,3-diaminopropionyl]–L-Ala–L-Arg–NH_2.

Human matrix metalloproteinase 7 (MMP-7, Matrilysin) [EC 3.4.24.23] is the smallest matrix metalloproteinase (MMP) (*1*, *2*). It lacks a carboxyl terminal haemopexin-like domain that is conserved in most MMPs. The molecular mass of the latent pro-form is 28 kDa, and that of the mature form is 19 kDa (*3*). MMP-7 is composed of a five-stranded β-sheet and three α-helices, and contains one zinc ion, essential for catalytic activity, and an additional zinc and two calcium ions that are considered necessary for stability (*4*). Like all other MMPs, it has two consensus sequences, HEXXHXXGXXH, in which three histidine residues chelate the catalytic zinc ion, and a methionine-containing turn (Met-turn). Hence, it is grouped in clan MA(M) (*5*). In recent years, target molecules through which MMP-7 exerts biological functions have become apparent, including heparin (*6*), heparan sulphate (*6*), cholesterol sulphate (*7–9*) and ErbB4 receptor (*10*). We reported the states of the tryptophyl residues of MMP-7 as determined by fluorescence examination (*11*) and the thermal stability and halophilic property of MMP-7 (*12*). We have proposed that Glu198 is the catalytically ionizable group responsible for acidic pK_e (pK_{e1}) and that an unidentified protein-bound water molecule could be that for alkaline pK_e (pK_{e2}), in the catalytic mechanism of MMP-7 (*13–15*). Throughout this article, the numbering of amino acid residues of pro-MMP-7 is applied to the mature MMP-7 beginning at Tyr78 (*16*).

MMP-7 has been detected in lesions of prostate (*17*), colon (*18*), brain (*19*), stomach (*20*), lung (*21*) and breast (*22*), and degrades extracellular material components, including gelatins of types I, III, IV and V, type IV basement membrane collagen, fibronectin, vitronectin, proteoglycan, laminin and elastin (*1–3*, *23–25*). This suggests that MMP-7 plays important roles in tumour invasion and metastasis. From this viewpoint, the development of MMP-7 inhibitors is considered to be of therapeutic benefit. We have reported inhibitory effects of alcohols (*26*), synthetic MMP inhibitors thiorphan and R-94138 (*27*), lignans (*28*) and green tea catechins (*29*, *30*) on MMP-7 activity in the hydrolysis of (7-methoxycoumarin-4-yl)acetyl–L-Pro–L-Leu–Gly–L-Leu-[N^3-(2,4-dinitrophenyl)-L-2,3-diaminopropionyl]-L-Ala–L-Arg–NH_2 (MOCAc-PLGL(Dpa)AR).

8-Alininonaphthalene 1-sulphonate (ANS) is a fluorescent probe widely used for the analysis of proteins (*31*, *32*). It has hydrophobic and hydrophilic groups. It emits large fluorescence energy when the

anilinonaphthalene group binds with proteins through hydrophobic interaction, whereas it does not emit fluorescence when the sulphonic group binds with proteins through electrostatic interaction (*33*). To explore the mechanism of the binding of MMP-7 with naturally occurring sulphated glycosaminoglycans, such as heparin, heparan sulphate and cholesterol sulphate, we think ANS is a useful probe due to the following reasons: (i) there is a possibility that the binding sites of MMP-7 for ANS are similar to those for the sulphated glycosaminoglycans and (ii) the binding of MMP-7 with ANS is more easily characterized than that for sulphated glycosaminoglycans. In this study, we describe the interaction of ANS and MMP-7 by examining the effects of ANS on MMP-7 activity and the effects of MMP-7 on ANS fluorescence.

Materials and Methods

Materials

MOCAc-PLGL(Dpa)AR (lot no. 491214, molecular mass 1093.2 Da) (*34*) and (7-methoxycoumarin-4-yl)acetyl-L-Pro–L-Leu–Gly (MOCAc-PLG; lot no. 510913, 501.54 Da) were purchased from Peptide Institute (Osaka, Japan). Their concentrations were determined by the denoted molecular weight. ANS (lot no. CM10-118, 299.34 Da) was from AnaSpec Inc. (San Jose, CA, USA). Its concentration was determined spectrophotometrically using the molar absorption coefficient at 350 nm, ε_{350}, of 5,000 $M^{-1}\,cm^{-1}$ (*35*, *36*). 3-[(1,1-Dimethyl-2-hydroxy-ethyl)amino]-2-hydroxypropane sulphonic acid (AMPSO) was from Wako Pure Chemical (Osaka, Japan). All other chemicals were purchased from Nacalai Tesque (Kyoto, Japan).

Expression and purification of MMP-7

Expression in *Escherichia coli* and purification of recombinant MMP-7 were carried out, as described previously (*37*, *38*). Briefly, mature MMP-7 (Tyr78–Lys250) was expressed in BL21(DE3) cells in the forms of inclusion bodies, solubilized with 6 M guanidine HCl, refolded with 1 M L-arginine and purified by sequential ammonium sulphate precipitation and heparin affinity column chromatography procedures of the refolded products. The concentration of MMP-7 was determined spectrophotometrically using the molar absorption coefficient at 280 nm, ε_{280}, of 31,800 $M^{-1}\,cm^{-1}$ (*37*, *38*).

Fluorometric analysis of the MMP-7-catalysed hydrolysis of MOCAc-PLGL(Dpa)AR

The reaction buffers were 50 mM acetate–NaOH buffer at pH 3.5 and 4.5, 50 mM MES–NaOH buffer at pH 5.5 and 6.5, 50 mM HEPES–NaOH buffer at pH 7.5 and 50 mM AMPSO–NaOH buffer at pH 8.5 and 9.5, each containing 10 mM $CaCl_2$. Pre-incubation (2,484 µl) was initiated by mixing 40 µl of the MMP-7 solution (2 µM in the reaction buffer), 0–250 µl of the ANS solution (5 mM in the reaction buffer), and 2,194–2,444 µl of the reaction buffer. After pre-incubation at 25°C for 10 min, the reaction was initiated by adding 16 µl of the substrate solution (234 µM) dissolved in DMSO. The initial concentrations of enzyme, MOCAc-PLGL(Dnp)AR and DMSO were 32 nM, 1.5 µM and 0.64% v/v, respectively. The reaction was measured by following the increase in fluorescence intensity at 393 nm with excitation at 328 nm with a Shimadzu RF-5300 fluorescence spectrophotometer (Kyoto, Japan) for 1 min at 25°C. The temperature was maintained in a range of ±0.2°C. The peptide bond of the Gly–L-Leu residues was cleaved by MMP-7, and the amount of the product, MOCAc -PLG, was estimated by fluorescence intensity by comparison with that of the MOCAc-PLG solution.

The increase in the fluorescence intensity at 393 nm due to the production of MOCAc-PLG (ΔFI_{393}) of the reaction mixture is affected by the presence of ANS. Hence, FI_{393} was measured with various concentrations of ANS in the absence and in the presence of 0.46 µM MOCAc-PLG. Based on the results, the ΔFI_{393} observed at x µM ANS was corrected by multiplying the following term:

$$\frac{[(FI_{393}\text{ of }0.46\ \mu\text{M MOCAc-PLG}) - (FI_{393}\text{ of buffer})]}{\left\{\begin{array}{l}[(FI_{393}\text{ of }0.46\ \mu\text{M MOCAc-PLG plus x }\mu\text{M ANS})\\ \quad -(FI_{393}\text{ of x }\mu\text{M ANS})]\end{array}\right\}}$$

The MMP-7-catalysed hydrolysis of the MOCAc-PLGL(Dpa)AR substrate was carried out under pseudo-first order conditions, where the initial concentration (1.5 µM) of the substrate was much lower than K_m (60 µM) (*28*). The Michaelis–Menten equation is, then, expressed as Eq. 1:

$$v_o = \left(\frac{k_{cat}}{K_m}\right)[E]_o[S]_o \cdots\cdots \quad (1)$$

where v_o, k_{cat}, $[E]_o$ and $[S]_o$ mean the initial reaction rate, the molecular activity, the initial enzyme concentration and the initial substrate concentration, respectively.

HPLC analysis of the MMP-7-catalysed hydrolysis of MOCAc-PLGL(Dpa)AR

Pre-incubation (950 µl) was initiated by mixing 16 µl of the MMP-7 solution (2 µM in the reaction buffer), 0, 25, 50, 100, 150 or 200 µl of the ANS solution (1 mM in 50 mM HEPES–NaOH buffer at pH 7.5) and 934, 909, 884, 834, 784 or 734 µl of the reaction buffer. After pre-incubation at 25°C for 10 min, the reaction was initiated by adding 50 µl of the MOCAc-PLGL(Dpa)AR (0–2.8 mM) dissolved in DMSO (the total volume of 1,000 µl) at 25°C. The initial concentrations of MMP-7, MOCAc-PLGL(Dpa)AR and DMSO were 32 nM, 0–140 µM and 5%, respectively. The reaction was stopped at an appropriate time by mixing 100 µl of the reaction solution with 400 µl of 1% trifluoroacetic acid (TFA). The mixture (100 µl) was then applied to reversed-phase HPLC performed on a TSKgel ODS-80Ts column [4.6 mm (inner diameter) × 150 mm] (Tosoh, Tokyo, Japan) equilibrated with 0.1% TFA. A linear gradient was generated from 20% to 70% (v/v) acetonitrile at a retention time of 5 min over 20 min at a flow-rate of 1.0 ml/min. The absorption of elutes was detected at 335 nm. The substrate and its two products, MOCAc-PLG and L(Dpa)AR, were separated (*12*). They were evaluated by the respective peak areas. The v_o was determined from the time course of the production of MOCAc-PLG. The kinetic parameters, k_{cat} and K_m, were determined based on the Michaelis–Menten equation using the nonlinear least-squares methods. The HPLC apparatus, consisting of a solvent delivery system CCPM, a UV monitoring system UV-8010, a computer control system PX-8010 and an integrator Chromatocorder 21, was from Tosoh.

Fluorometric analysis of ANS

Pre-incubation (1,000 µl) was initiated by mixing 100 µl of the ANS solution (250 µM in the reaction buffer), 400 µl of the reaction buffer and 500 µl of the MMP-7 solution (1,000 nM in the reaction buffer) at 25°C for 10 min. After the pre-incubation, the fluorescence spectra were measured with excitation at 380 nm and emission at 400–600 nm with a Shimadzu RF-5300PC fluorescence spectrophotometer at 25°C.

CD measurement

Pre-incubation (500 µl) was initiated by mixing 164 µl of the reaction buffer and 336 µl of the MMP-7 solution (10.4 µM in the reaction buffer) at 25°C for 10 min. After the pre-incubation, the CD spectra were measured using 2-mm cell with Jasco J-820 (Tokyo, Japan) spectropolarimeter equipped with a Peltier system of cell temperature control. Ellipticity was reported as mean residue molar ellipticity [θ] (deg cm^2 $dmol^{-1}$). The spectrometer conditions were: spectral range 200–270 nm; 100 mdeg sensitivity; 0.2 nm resolutions; 0.2 s response time; 50 nm min^{-1} scan rate; and 5 accumulations. The control baseline was obtained with solvent and all the components without the proteins.

Results

Inhibition of MMP-7 activity by ANS

Figure 1A shows the effects of increasing concentrations of ANS on MMP-7 activity in the hydrolysis of MOCAc-PLGL(Dpa)AR. MMP-7 (32 nM) and ANS

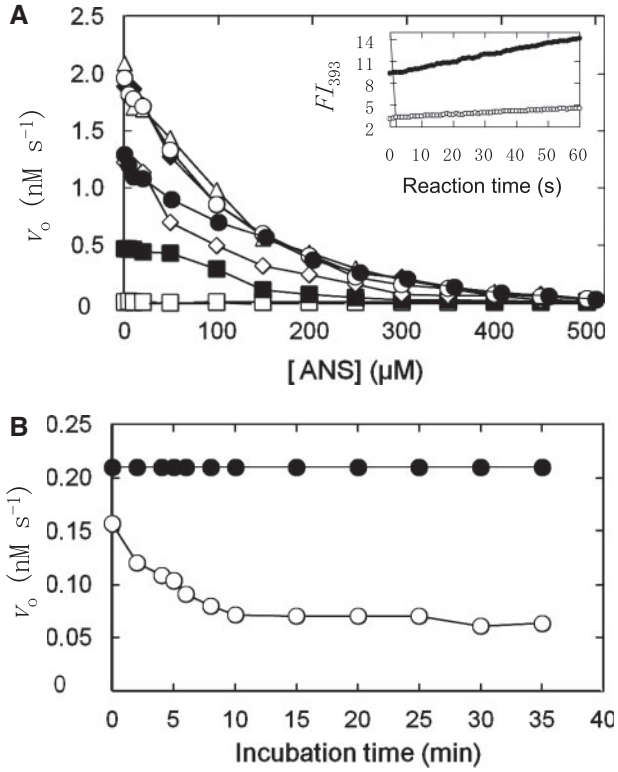

Fig. 1 Fluorometoric analysis of inhibition of the MMP-7-catalysed hydrolysis of MOCAc-PLGL(Dpa)AR by ANS. (A) Effect of pH and ANS concentration on the initial reaction rate, v_o. Pre-incubation of ANS and MMP-7 was carried out at 25°C for 10 min. The reaction was carried out with 32 nM MMP-7, 1.5 μM MOCAc-PLGL(Dpa)AR, 0–500 μM ANS and 0.64% DMSO at pH 3.5 (open square), 4.5 (solid square), 5.5 (open diamond), 6.5 (solid diamond), 7.5 (open triangle), 8.5 (open circle) and 9.5 (solid circle) at 25°C. Inset shows the time-dependency of the reaction with 200 μM ANS (open circle) or without it (solid circle) at pH 7.5 at 25°C. (B) Effect of pre-incubation time on v_o. Pre-incubation was carried out at 25°C for 0–35 min. The reaction was carried out with 50 μM ANS (open circle) or without it (solid circle) at pH 7.5 at 25°C. One of the representative experiments is shown.

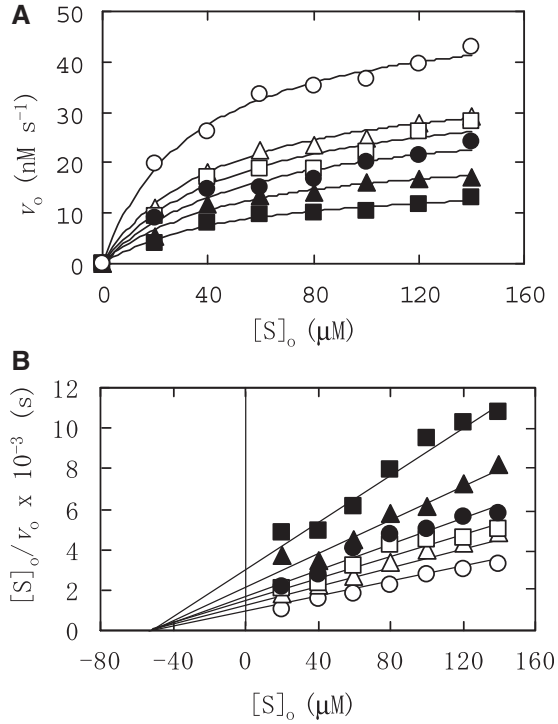

Fig. 2 HPLC analysis of inhibition of the MMP-7-catalysed hydrolysis of MOCAc-PLGL(Dpa)AR by ANS. The reaction was carried out with 32 nM MMP-7, 0–140 μM MOCAc-PLGL(Dpa)AR, 0 (open circle), 25 (open triangle), 50 (open square), 100 (solid circle), 150 (solid triangle) or 200 (solid square) μM ANS, and 5% DMSO at 25°C, and stopped at an appropriate time. (A) Effect of the initial substrate concentrations, $[S]_o$ on v_o. Solid line represents the best fit of the Michaelis–Menten equation using the non-linear least-squares methods. (B) Hanes–Woolf plot. One of the representative experiments is shown.

(0–500 μM) were pre-incubated at pH 3.5–9.5 at 25°C for 10 min followed by the reaction at the same pH at 25°C. As shown in the inset, the fluorescence increased linearly with increasing reaction time (inset for without ANS and with 200 μM ANS at pH 7.5; data not shown for other ANS concentrations and/or other pH). At pH 3.5, MMP-7 did not exhibit activity. At pH 6.5–8.5, it exhibited the highest activity. It is known that MMP-7 has a bell-shaped pH-dependence activity with the pK_{e1} and pK_{e2} values of 4.2–4.6 and 9.7–9.8 (*13–15*). The pH dependence of activity observed in the absence of ANS was in good agreement with the previous results. At pH 4.5–9.5, the initial reaction rates decreased with increasing ANS concentration, indicating that ANS inhibits MMP-7 activity. The ANS concentrations giving 50% inhibition (IC_{50} values) at pH 4.5, 5.5, 6.5, 7.5, 8.5, 9.5 were 120, 64, 90, 96, 92 and 135 μM, respectively. On the other hand, sodium sulphate (0–500 μM) did not inhibit MMP-7 activity (data not shown) suggesting that anilinonaphthalene group of ANS is required for the inhibition of MMP-7 activity.

Figure 1B shows the effects of pre-incubation time on MMP-7 activity. MMP-7 (32 nM) and ANS (50 μM) were pre-incubated at pH 7.5 at 25°C for 0–35 min followed by the reaction at pH 7.5 at 25°C. The initial reaction rates decreased with increasing pre-incubation time and reached the minimum at 10 min, indicating that ANS exhibits slow-binding inhibition of MMP-7.

Inhibitory manner of ANS against MMP-7 activity

To determine k_{cat} and K_m of MMP-7 in the hydrolysis of MOCAc-PLGL(Dpa)AR separately, the initial reaction rates in the absence and in the presence of ANS were measured. It was necessary to increase the concentration of MOCAc-PLGL(Dpa)AR up to 140 μM that is higher than the K_m value (60 μM) (*28*), and fluorescence detection was not available because of the inner-filter effect of the substrate. Accordingly, the products were detected by HPLC on a TSK-gel ODS column (*12*). All the plots showed saturated profiles (Fig. 2A). The plot of $[S]_o/v_o$ versus $[S]_o$ (Hanes–Woolf plot) in the absence and in the presence of ANS showed non-parallel lines intersecting at the *X*-axis, suggesting that the K_m value was 52 μM and that the inhibition is non-competitive (Fig. 2B). The k_{cat} values with 0, 25, 50, 100, 150 and 200 μM were

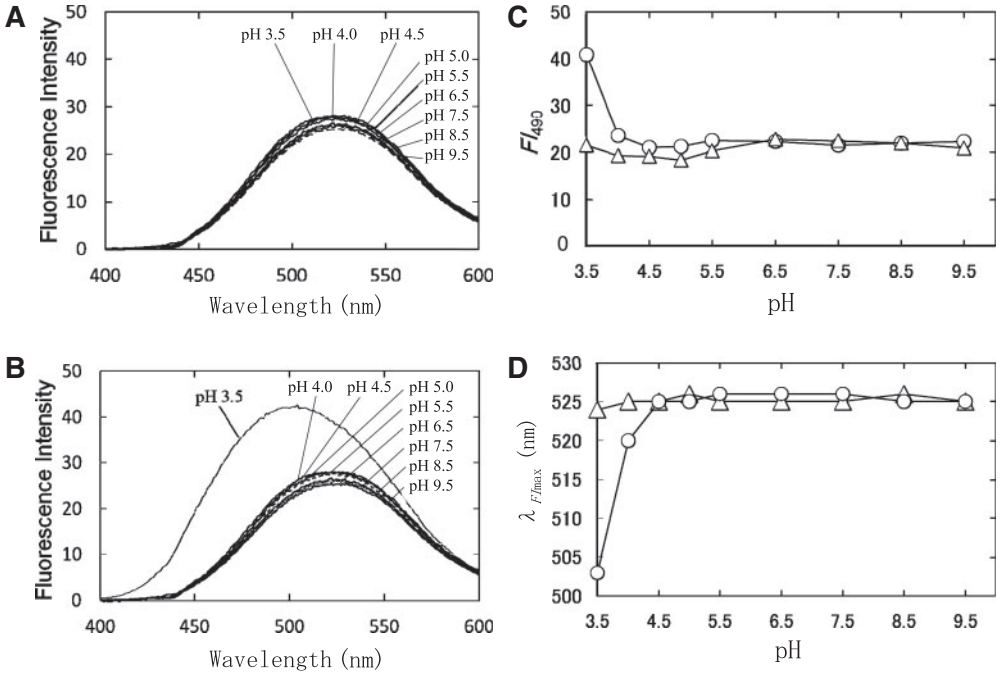

Fig. 3 Effect of pH and MMP-7 on the fluorescence of ANS. Fluorescence spectra were measured with excitation at 380 nm and emission at 400–600 nm for 25 μM ANS in 50 mM acetate–NaOH buffer at pH 3.5, 4.0 and 4.5, 50 mM MES–NaOH buffer at pH 5.0, 5.5 and 6.5, 50 mM HEPES–NaOH buffer at pH 7.5 and 50 mM AMPSO–NaOH buffer at pH 8.5 and 9.5, each containing 10 mM $CaCl_2$ at 25°C. (A) Fluorescence spectra in the absence of MMP-7. (B) Fluorescence spectra in the presence of 500 nM MMP-7. (C) Fluorescence intensity at 490 nm (FI_{490}). (D) Wavelength giving the maximum fluorescence (λ_{FImax}). FI_{490} (C) and λ_{FImax} (D) of ANS in the presence of 500 nM MMP-7 (open circle) and in its absence (open triangle) were plotted against pH. One of the representative experiments is shown.

determined to be 1.6 ± 0.1, 1.2 ± 0.1, 1.1 ± 0.1, 1.0 ± 0.1, 0.7 ± 0.1 and $0.5 \pm 0.1\,s^{-1}$, respectively. Based on this, the reaction rate can be described as Eq. 2:

$$v_o = \frac{k_{cat}[E]_o[S]_o}{\left(K_m + [S]_o\right)\left(1 + \frac{[I]_o}{K_i}\right)} \cdots\cdots \quad (2)$$

where $[I]_o$ is the initial inhibitor concentration and K_i is the inhibitor constant. The K_i value of ANS at pH 7.5 was calculated to be 110 ± 20 μM from Eq. 2, which was similar to the IC_{50} at pH 7.5 (96 μM) as described above.

Effects of MMP-7 on the fluorescence of ANS

Fluorescence spectra of ANS in the absence and in the presence of MMP-7 were measured (Fig. 3). The shape of the fluorescence spectra of ANS measured at pH 3.5–9.5 in the absence of MMP-7 were almost the same, although the intensity of those at pH 3.5–4.5 was slightly higher than that of those at pH 5.0–9.5 (Fig. 3A). On the other hand, the spectrum observed at pH 3.5 in the presence of 500 nM MMP-7 was drastically changed in comparison of that in its absence (Fig. 3B): the fluorescence intensity at 490 nm (FI_{490}) with 500 nM MMP-7 was 200% of that without it (Fig. 3C), and the wavelength giving the maximum fluorescence (λ_{FImax}) with 500 nM MMP-7 was shorter by 20 nm than that without it. On the other hand, there were no differences in FI_{490} (Fig. 3C) and λ_{FImax} (Fig. 3D) among the spectra without MMP-7 at pH 3.5–9.5 and those with 500 nM MMP-7 at pH 4.0–9.5. These results suggest that the anilinonaphthalene group of ANS does not bind with hydrophobic regions of MMP-7 at pH 4.0–9.5, but binds at pH 3.5.

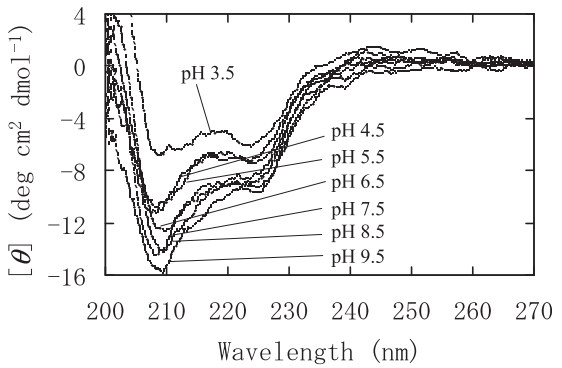

Fig. 4 Effect of pH on the CD spectra of MMP-7. CD spectra were measured for 7.0 μM MMP-7 in 50 mM acetate–NaOH buffer at pH 3.5 and 4.5, 50 mM MES–NaOH buffer at pH 5.5 and 6.5, 50 mM Tris–HCl buffer at pH 7.5 and 50 mM AMPSO–NaOH buffer at pH 8.5 and 9.5, each containing 10 mM $CaCl_2$ at 25°C. One of the representative experiments is shown.

Effects of pH on the CD spectra of MMP-7

CD spectra of MMP-7 in the absence of ANS were measured at pH 3.5–9.5 (Fig. 4). Each spectrum was characterized by negative ellipticities at around 206–230 nm with the peaks around 208 and 225 nm, indicating that there is little difference in secondary

structure. The ellipticities at 206–230 nm at pH 3.5 were slightly smaller than those at pH 4.5–9.5. The contents of α-helix, β-sheet, calculated based on the reference spectra (*39*), at pH 3.5 were 31, 31 and 38%, respectively, and those at pH 4.5–9.5 in average were 31, 34 and 35%, respectively. This suggests that MMP-7 did not receive a drastic structural change at pH 3.5.

Effects of alcohols on the fluorescence of ANS

Fluorescence spectra of ANS in the presence of ethanol and 2-propanol were measured (Fig. 5). The fluorescence intensity increased with increasing concentrations of ethanol (Fig. 5A) and 2-propanol (Fig. 5B). FI_{490} of ANS increased with increasing alcohol concentrations (Fig. 5C). $\lambda_{FI\max}$ of ANS decreased with increasing alcohol concentrations and reached 487 nm at 80% ethanol and 482 nm at 80% 2-propanol (Fig. 5D). Relative FI_{490} of the ANS solution in the presence of ethanol was defined as the relative value of FI_{490} to that without ethanol. Figure 5E shows relative FI_{490} of the ANS solution in the presence of dielectric constant (D) of the solution, calculated as described previously (*40*). The relative FI_{490} of 2.0 of ANS, which was observed in the presence of 500 nM MMP-7 at pH 3.5, corresponds to the D value of 72.

Discussion

Mechanism of inhibition of MMP-7 activity by ANS

We have analysed the inhibition of MMP-7 activity by various compounds (*26–30*). Alcohols inhibit MMP-7 activity competitively with K_i values of 0.66–4.80 μM (*26*). It is suggested that MMP-7 has the inhibitor-binding site for alcohol with the size large enough to accommodate the length of four-carbon chain and the bulk of tertiary alcohols (*26*). Thiorphan and R-94318, which were originally designed as inhibitors of enkephalinase and gelatinase, respectively, inhibit MMP-7 activity competitively with the K_i values of 11.2 and 7.65 μM, respectively (*27*). Lignans also inhibit MMP-7 activity competitively with the IC_{50} or K_i values of 50–280 μM (*28*). It is suggested that non-polar character of the dibenzylbutyrolactone structure is important in the inhibition (*28*). Green tea catechins with the galloyl group inhibit MMP-7 activity non-competitively, with the K_i

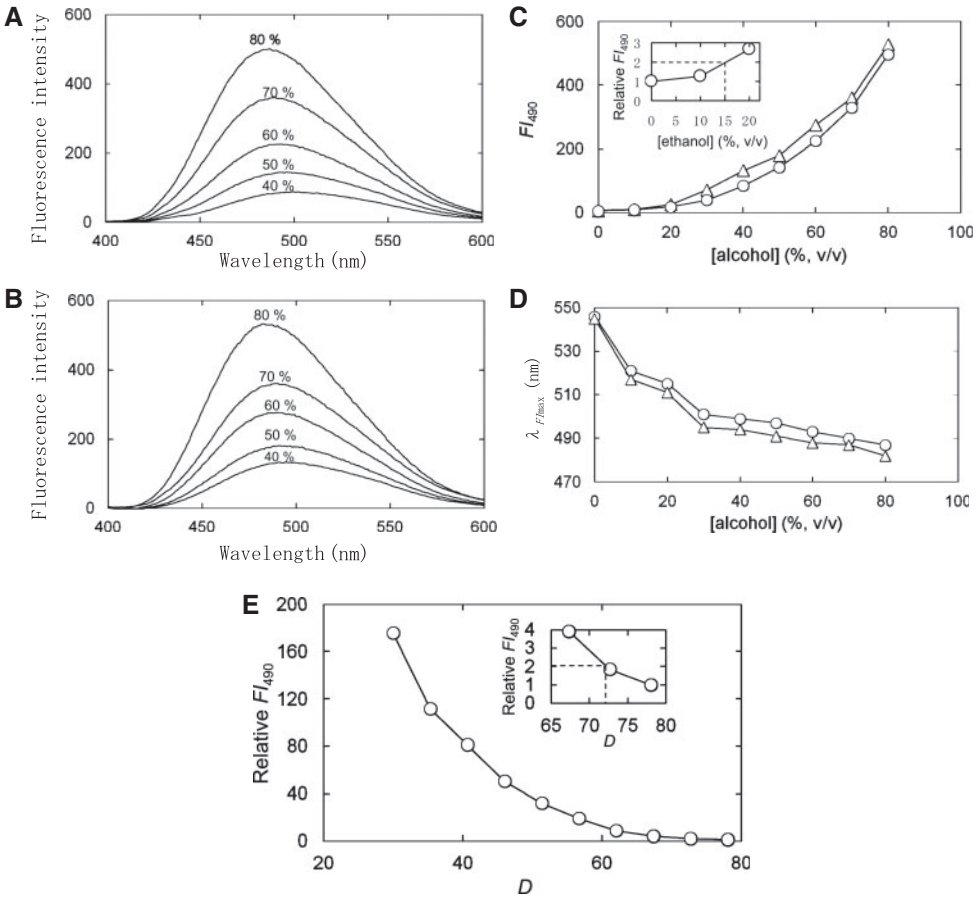

Fig. 5 Effect of alcohols on the fluorescence of ANS. Fluorescence spectra were measured with excitation at 380 nm and emission at 400–600 nm for 5 μM ANS in 50 mM HEPES–NaOH, 10 mM of $CaCl_2$, pH 7.5 with various concentrations of alcohols at 25°C. (A) Fluorescence spectra with 40, 50, 60, 70 and 80% of ethanol. (B) Fluorescence spectra with 40, 50, 60, 70 and 80% of 2-propanol. (C) Fluorescence intensity at 490 nm (FI_{490}). Relative FI_{490} was defined as the relative value of FI_{490} in the presence of ethanol to the value in its absence. The broken lines in the inset mean that 15% ethanol corresponds to relative FI_{490} of 2.0. (D) Wavelength giving the maximum fluorescence ($\lambda_{FI\max}$). Symbols for alcohols (C and D): ethanol, open circle; 2-propanol, open triangle. (E) Relative FI_{490}. Dielectric constant, D, is calculated according to Eq. 2. The broken lines in the inset mean that relative fluorescence intensity of 2.0 corresponds to the D value of 72.

values of 0.47–1.65 μM (*29*). In this study, it is demonstrated that ANS inhibits MMP-7 activity in a non-competitive manner with the K_i value of 110 ± 20 μM (Fig. 2). The degree of inhibition depends on the time for pre-incubation of ANS and MMP-7 (Fig. 1B). ANS fluorescence is not changed by the addition of MMP-7 at pH 4.0–9.5 (Fig. 3), suggesting that the sulphonic, but not anilinonaphthalene, group of ANS binds with MMP-7 through hydrophilic interaction. From these results, there is an interesting tendency speculated that hydrophobic inhibitors inhibit MMP-7 activity competitively, while hydrophilic inhibitors inhibit it non-competitively.

Considering the cleavage site of MOCAc -PLGL(Dpa)AR by MMP-7 and the structure of thiorphan (*27*), the binding of substrate and inhibitors to the S1′ pocket of the active site is the most important. It is thought that the S1′ pocket is hydrophobic and prefer hydrophobic residues, such as Leu, Phe and Trp, but is not large enough to accommodate the anilinonaphthalene group of ANS.

Binding of MMP-7 with ANS

The pI value of MMP-7 is 5.9 (*3*). The pK_a value of the sulphonic group of ANS is less than 2 (*41*, *42*). Considering that (i) the sulphonic group is negatively charged at pH 4.0–9.5, (ii) the fluorescence of ANS is not increased by the addition of MMP-7 at pH 4.0–9.5 and (iii) MMP-7 binds with heparin, heparan sulphate and cholesterol sulphate (*6–9*), it is suggested that ANS binds with the positively charged surface regions of MMP-7. MMP-7 has 11 Lys residues and 8 Arg residues. Figure 6 shows overall structure of MMP-7. When MMP-7 is viewed with the active site on the centre, only three Lys residues (Lys235, Lys239 and Lys243) and two Arg residues (Arg143 and Arg180) are on the surface, while the reverse side shows Lys and Arg residues all over the surface (*4*, *6*) (Fig. 6), suggesting that ANS could bind with the regions far from the active site of MMP-7. Regarding this, it was reported that the binding site of MMP-7 with cholesterol sulphate is located on the other side of the active site (*7*), and that the amino acid residues of MMP-7 involved in the binding to cholesterol sulphate are Ile106, Arg110, Arg128, Trp132, Arg248, Lys249 and Lys250 (Fig. 6B) (*8*). In this article, we speculate that several cholesterol sulphate molecules bind with one MMP-7 molecule because five basic residues (Arg110, Arg128, Arg248, Lys249 and Lys250) contribute to the binding (*8*). Although the binding sites of MMP-7 for ANS have not been identified, we speculate that several ANS molecules bind with one MMP-7 molecule. It was also reported that MMP-7 that binds with negatively charged liposomes retains the activity, whereas while MMP-7 that binds with positively charged liposomes loses it (*43*). Therefore, in a physiological condition, MMP-7 might bind with sulphated glycosaminoglycans on the surface of tumour cells through the basic regions far from the active site. Identification of the binding sites of MMP-7 for ANS is the next research subject.

FI_{490} of ANS with 500 nM MMP-7 and without alcohol at pH 3.5 was 200% of that without MMP-7 and

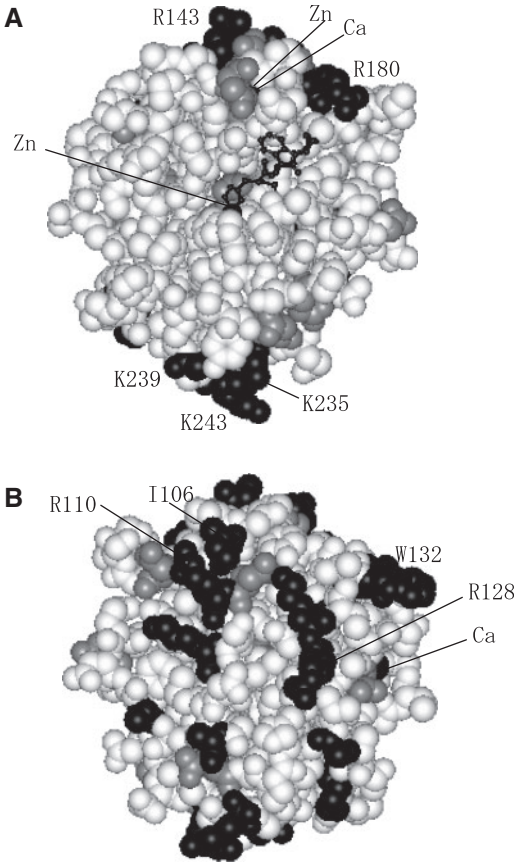

Fig. 6 Overall structure of MMP-7. The MMP-7-hydroxymate inhibitor complex is based on the Protein Data Bank no. 1MMQ (*4*). MMP-7 residues (Tyr78–Lys243) are represented by a CPK model. Black, Lys, Arg, Ile86 or Trp132; Gray, Asp or Glu. Arg244, Ser245, Asn246, Ser247, Arg248, Lys249 and Lys250 are not shown because they are not contained in 1MMQ. The hydroxymate inhibitor is represented by a ball and stick model. (A) MMP-7 viewed with the active site at the centre. (B) MMP-7 viewed from the opposite side.

alcohol at pH 3.5 (Fig. 3C). FI_{490} of ANS with 15% ethanol without MMP-7 at pH 7.5 was 200% of that without alcohol and MMP-7 at pH 7.5 (Fig. 5C). This increase in FI_{490} of ANS corresponds to the dielectric constant (D) value of 72 (Fig. 5E), suggesting that the environment at the binding sites of MMP-7 for ANS at pH 3.5 is more hydrophobic than water ($D = 78$).

ANS has been used to explore conformational changes of proteins as a hydrophobic probe (*44–48*): in the complex of ANS with arginine kinase (*44*) or bromelain (*45*), ANS fluorescence was first increased and then decreased with increasing concentration of guanidine hydrochloride, suggesting the presence of a partially unfolded intermediate between the native and the fully unfolded states. In the complex of ANS with citrate synthase, ANS fluorescence was increased by the addition acetyl–CoA or ATP, which is ascribed to the ligand-induced conformational change (*46*). In the complex of ANS with phospholipase A2, ANS fluorescence was increased by the addition of Ca^{2+}, which is ascribed to the binding of Ca^{2+} with the active-site aspartate residue (*47*). In the complex of ANS with interleukin-6 (IL-6), ANS fluorescence was

increased by disrupting the intramolecular disulphide by dithiothreitol (*48*). In this study, MMP-7 did not exhibit activity at pH 3.5 after pre-incubation without ANS for 10 min at pH 3.5 (Fig. 1A). The fluorescence of ANS was increased by the addition of MMP-7 at pH 3.5, but not at pH 4.0–9.5 (Fig. 3). This can be explained by that at pH 3.5, MMP-7 receives a structural change and the anilinonaphthalene group of ANS binds with hydrophobic regions of MMP-7 although the degree of structural change of MMP-7 at pH 3.5 is thought to be small according to the results with CD spectra of MMP-7 (Fig. 4). Characterization of this structural change of MMP-7 and identification of the binding sites of MMP-7 for the anilinonaphthalene group of ANS are also important research subjects.

Funding
Grants-in-Aid for Scientific Research, Japan Society for the Promotion of Science (nos. 17380065 and 20380061 to K.I., partial).

Conflict of interest
None declared.

References

1. Woessner, J.F. Jr (1991) Matrix metalloproteinases and their inhibitors in connective tissue remodeling. *FASEB J.* **5**, 2145–2154
2. Nagase, H. and Woessner, J.F. Jr (1999) Matrix metalloproteinases. *J. Biol. Chem.* **274**, 21491–21494
3. Woessner, J.F. Jr and Taplin, C.J. (1988) Purification and properties of a small latent matrix metalloproteinase of the rat uterus. *J. Biol. Chem.* **263**, 16918–16925
4. Browner, M.F., Smith, W.W., and Castelhano, A.L. (1995) Matrilysin-inhibitor complexes: common themes among metalloproteases. *Biochemistry* **34**, 6602–6610
5. Rawlings, N.D., Morton, N.D., Kok, F.R., Kong, C.Y., and Barrett, A.J. (2008) MEROPS: the peptidase database. *Nucleic Acids Res.* **36**, D320–D325
6. Yu, W.-H. and Woessner, J.F. Jr (2000) Heparan sulfate proteoglycans as extracellular docking molecules for matrilysin (matrix metalloproteinase 7). *J. Biol. Chem.* **275**, 4183–4191
7. Yamamoto, K., Higashi, S., Kioi, M., Tsunezumi, J., Honke, K., and Miyazaki, K. (2006) Binding of active matrilysin to cell surface cholesterol sulfate is essential for its membrane-associated proteolytic action and induction of homotypic cell adhesion. *J. Biol. Chem.* **281**, 9170–9180
8. Higashi, S., Oeda, M., Yamamoto, K., and Miyazaki, K. (2008) Identification of amino acid residues of matrix metalloproteinase 7 essential for binding to cholesterol sulfate. *J. Biol. Chem.* **283**, 35735–35744
9. Yamamoto, K., Miyazaki, K., and Higashi, S. (2010) Cholesterol sulphate alters substrate preference of matrix metalloproteinase-7 and promotes degradations of pericellular laminin-332 and fibronectin. *J. Biol. Chem.* **285**, 28862–28873
10. Lynch, C.C., Vargo-Gogola, T., Martin, M.D., Fingleton, B., Crawford, H.C., and Matrisian, L.M. (2007) Matrix metalloproteinase 7 mediates mammary epithelial cell tumorigenesis through the ErbB4 receptor. *Cancer Res.* **57**, 6760–6767
11. Inouye, K., Tanaka, H., and Oneda, H. (2000) States of tryptophyl residues and stability of recombinant human matrix metalloproteinase 7 (matrilysin) as examined by fluorescence. *J. Biochem.* **128**, 363–369
12. Oneda, H. and Inouye, K. (2000) Effects of dimethyl sulfoxide, temperature, and sodium chloride on the activity of human matrix metalloproteinase 7 (matrilysin). *J. Biochem.* **128**, 785–791
13. Muta, Y., Oneda, H., and Inouye, K. (2005) Anomalous pH-dependence of the activity of human matrilysin (matrix metalloproteinase-7) as revealed by nitration and amination of its tyrosine residues. *Biochem. J.* **386**, 263–270
14. Muta, Y. and Inouye, K. (2011) Tyr219 of human matrix metalloproteinase 7 (MMP-7) is not critical for catalytic activity, but is involved in the broad pH-dependence of the activity. *J. Biochem.* **150**, 183–188
15. Takeharu, H., Yasukawa, K., and Inouye, K. (2011) Thermodynamic analysis of ionizable groups involved in the catalytic mechanism of human matrix metalloproteinase 7 (MMP-7). *Biochim. Biophys. Acta* **1814**, 1940–1946
16. Crabbe, T., Willenbrock, F., Eaton, D., Hynds, P., Carne, A.F., Murphy, G., and Docherty, A.J. (1992) Biochemical characterization of matrilysin. Activation conforms to the stepwise mechanisms proposed for other matrix metalloproteinases. *Biochemistry* **31**, 8500–8507
17. Pajouh, M.S., Nagle, R.B., Brethnach, R., Finch, J.S., Brawer, M.K., and Bowden, G.T. (1991) Expression of metalloproteinase genes in human prostate cancer. *J. Cancer Res. Clin. Oncol.* **117**, 114–150
18. Yoshimoto, M., Itoh, F., Yamamoto, H., Hinoda, Y., Imai, K., and Yachi, A. (1993) Expression of MMP-7 (PUMP-1) mRNA in human colorectal cancers. *Int. J. Cancer* **54**, 614–618
19. Nakano, A., Tani, E., Miyazaki, K., Yamamoto, Y., and Furuyama, J. (1995) Matrix metalloproteinases and tissue inhibitors of metalloproteinases in human gliomas. *J. Neurosurg.* **83**, 298–307
20. Adachi, Y., Itoh, F., Yamamoto, H., Matsuno, K., Arimura, Y., Kusano, M., Endo, T., Hinoda, Y., Oohara, M., Hosokawa, M., and Imai, K. (1998) Matrix metalloproteinase matrilysin (MMP-7) participates in the progression of human gastric and esophageal cancers. *Int. J. Oncol.* **13**, 1031–1035
21. Muller, D., Breathnach, R., Engelmann, A., Millon, R., Bronner, G., Flesch, H., Dumont, P., Eber, M., and Abecassis, J. (1991) Expression of collagenase-related metalloproteinase genes in human lung or head and neck tumors. *Int. J. Cancer* **48**, 550–556
22. Heppner, K.J., Matrisian, L.M., Jensen, R.A., and Rodgers, W.H. (1996) Expression of most matrix metalloproteinase family members in breast cancer represents a tumor-induced host response. *Am. J. Pathol.* **149**, 273–282
23. Miyazaki, K., Hattori, Y., Umenishi, F., Yasumitsu, H., and Umeda, M. (1990) Purification and characterization of extracellular matrix-degrading metalloproteinase, matrin (pump-1), secreted from human rectal carcinoma cell line. *Cancer Res.* **50**, 7758–7764
24. Imai, K., Shikata, H., and Okada, Y. (1995) Degradation of vitronectin by matrix metalloproteinases-1, -2, -3, -7 and -9. *FEBS Lett.* **369**, 249–251
25. Murphy, G., Cockett, M.I., Ward, R.V., and Docherty, A.J. (1991) Matrix metalloproteinase degradation of elastin, type IV collagen, and proteoglycan: a

quantitative comparison of the activities of 95 kDa and 72 kDa gelatinases, stromelysins-1 and -2, and punctuated metalloproteinase (PUMP). *Biochem. J.* **277**, 277–279
26. Muta, Y., Oneda, H., and Inouye, K. (2004) Inhibitory effects of alcohols on the activity of human matrix metalloproteinase 7 (matrilysin). *Biosci. Biotechnol. Biochem.* **68**, 2649–2652
27. Oneda, H. and Inouye, K. (2001) Interactions of human matrix metalloproteinase 7 (matrilysin) with the inhibitors thiorphan and R-94138. *J. Biochem.* **129**, 429–435
28. Muta, Y., Oyama, S., Umezawa, T., Shimada, M., and Inouye, K. (2004) Inhibitory effects of lignans on the activity of human matrix metalloproteinase 7 (matrilysin). *J. Agric. Food Chem.* **52**, 5888–5894
29. Oneda, H., Shiihara, M., and Inouye, K. (2003) Inhibitory effects of green tea catechins on the activity of human matrix metalloproteinase 7 (matrilysin). *J. Biochem.* **133**, 571–576
30. Miyake, T., Yasukawa, K., and Inouye, K. (2011) Analysis of the mechanism of inhibition of human matrix metalloproteinase 7 (MMP-7) activity by green tea catechins. *Biosci. Biotechnol. Biochem.* **75**, 1564–1569
31. Hawe, A., Sutter, M., and Jiskoot, W. (2007) Extrinsic fluorescent dyes as tools for protein characterization. *Pharm. Res.* **25**, 1487–1499
32. Stryer, L. (1965) The interaction of a naphthalene dye with apomyoglobin and apohemoglobin. A fluorescent probe of non-polar binding sites. *J. Mol. Biol.* **13**, 482–495
33. Slavik, J. (1982) Anilinonaphthalene sulfonate as a probe of membrane composition and function. *Biochim. Biophys. Acta* **694**, 1–25
34. Knight, C.G., Willenbrock, F., and Murphy, G. (1992) A novel coumarin-labelled peptide for sensitive continuous assays of the matrix metalloproteinase. *FEBS Lett.* **296**, 263–266
35. Khurana, R. and Udgaonkar, J.B. (1994) Equilibrium unfolding studies of barstar: evidence for an alternative conformation which resembles a molten globule. *Biochemistry* **33**, 106–115
36. Haq, S.K., Rasheedi, S., and Khan, R.H. (2002) Characterization of a partially folded intermediate of stem bromelain at low pH. *Eur. J. Biochem.* **269**, 47–52
37. Oneda, H. and Inouye, K. (1999) Refolding and recovery of recombinant human matrix metalloproteinase 7 (matrilysin) from inclusion bodies expressed by *Escherichia coli*. *J. Biochem.* **126**, 905–911
38. Muta, Y., Yasui, N., Matsumiya, Y., Kubo, M., and Inouye, K. (2010) Expression in *Escherichia coli*, refolding, and purification of the recombinant mature form of human matrix metalloproteinase 7 (MMP-7). *Biosci. Biotechnol. Biochem.* **74**, 2515–2517
39. Chen, Y.H., Yang, J.T., and Chau, K.H. (1974) Determination of the helix and β form of proteins in aqueous solution by circular dichroism. *Biochemistry* **13**, 3350–3359
40. Inouye, K., Lee, S.-B., Nambu, K., and Tonomura, B. (1997) Effects of pH, temperature, and alcohols on the remarkable activation of thermolysin by salts. *J. Biochem.* **122**, 358–364
41. Gasymov, O.K. and Glasgow, B.J. (2007) ANS fluorescence: potential to augment the identification of the external binding sites of proteins. *Biochim. Biophys. Acta* **1774**, 403–411
42. Andújar-Sánchez, M., Martínez-Rodríguez, S., Heras-Vázquez, F.J., Clemente-Jiménez, J.M., Rodríguez-Vico, F., and Jara-Pérez, V. (2006) Binding studies of hydantoin racemase from *Sinorhizobium meliloti* by calorimetric and fluorescence analysis. *Biochim. Biophys. Acta* **1764**, 292–298
43. Ganguly, B., Banerjee, J., Elegbede, A.I., Klocke, D.J., Mallik, S., and Srivastava, D.K. (2007) Intrinsic selectivity in binding of matrix metalloproteinase-7 to differently charged lipid membranes. *FEBS Lett.* **581**, 5723–5726
44. Tang, H.M. and Yu, H. (2005) Intermediate studies on refolding of arginine kinase denatured by guanidine hydrochloride. *Biochem. Cell Biol.* **83**, 109–114
45. Haq, S.K., Rasheedi, S., and Khan, R.H. (2002) Characterization of a partially folded intermediate of stem bromelain at low pH. *Eur. J. Biochem.* **269**, 47–52
46. Kollmann-Koch, A. and Eggerer, H. (1989) Ligand-induced conformational changes of citrate synthase studied with the fluorescent probe 8-anilinonaphthalene 1-sulfonate. *Eur. J. Biochem.* **185**, 441–447
47. Van Eijk, J.H., Verheij, H.M., and de Haas, G.H. (1984) Interaction of native and modified *Naja melanoleuca* phospholipases A_2 with the fluorescent probe 8-anilinonaphtalene-1-sulfonate. *Eur. J. Biochem.* **140**, 407–413
48. Zhang, J.G., Matthews, J.M., Ward, L.D., and Simpson, R.J. (1997) Disruption of disulfide bonds of recombinant murine interleukin-6 induces formation of a partially unfolded state. *Biochemistry* **36**, 2380–2389